

Flavor Hierarchy from Smooth Confinement

Yuta Hamada* and Juven Wang†

**Theory Center, IPNS, High Energy Accelerator Research Organization (KEK),
1-1 Oho, Tsukuba, Ibaraki 305-0801, Japan*

**Graduate University for Advanced Studies (Sokendai), 1-1 Oho, Tsukuba,
Ibaraki 305-0801, Japan*

**Department of Physics, Harvard University, Cambridge, MA 02138 USA*

†*Center of Mathematical Sciences and Applications, Harvard University, MA 02138, USA*

Abstract

We present a model to explain the Standard Model flavor hierarchy. Our model is based on explicit smooth confinement (namely confinement without chiral symmetry breaking in a supersymmetric gauge theory) at an intermediate energy scale, before the electroweak symmetry breaking by the Higgs condensation at lower energy. In our context, the smooth confinement preserves the $SU(3)$ and the chiral $SU(2)_L \times U(1)_Y$ symmetry in a supersymmetric Standard Model, while this internal symmetry becomes dynamically gauged in the end. In contrast to Razamat-Tong's symmetric mass generation model also preserving the $G_{SM} \equiv SU(3)_C \times SU(2)_L \times U(1)_Y$ internal symmetry, our model introduces different matter contents with a different kind of superpotential deformation irrelevant at UV, which further induces Yukawa-Higgs terms marginal at IR, breaking the G_{SM} down to $SU(3)_C$ and the electromagnetic $U(1)_{EM}$ only when Higgs condenses. In our model, the IR fermions in the first and second families are composite of UV fields, while the third family elementary fermions match between UV and IR. The smallness of the first and second family fermion masses is explained by the exponential hierarchy between the cutoff scale and the smooth confinement scale via dimensional transmutation. As a result, our UV Lagrangian only contains the natural parameters close to the order one.

*E-mail: yhamada@post.kek.jp

†E-mail: jw@cmsa.fas.harvard.edu

1 Introduction

One of the mysteries of the Standard Model (SM) is the flavor hierarchical structure. The observed lightest charged fermion in our world is the electron, and its mass is 511 keV [1]. On the other hand, the heaviest one is the top quark, and its mass is about 172 GeV [2]. Both fermions acquire masses from the Yukawa coupling with the condensation of the Higgs field. Therefore, the huge difference in the fermion masses indicates that the Yukawa coupling has a hierarchical structure. More concretely, the ratio between the electron and top Yukawa coupling is 3×10^5 . Why is there such a large flavor hierarchy?

One of the known solutions was provided by Froggatt and Nielsen in Ref. [3]. They introduced a flavor-dependent U(1) symmetry and a scalar field called flavon charged under it. The small parameter is introduced if the vev of the Higgs is smaller than the cutoff scale.

In this work, we present a new solution, inspired by the dynamics of the nonperturbative strong coupling of gauge theory, known as the smooth confinement (or the s-confinement [4, 5], which means confinement without chiral symmetry breaking in the supersymmetry context). The idea is that we hypothesize some matter fields of the (supersymmetric) SM at IR can be obtained as the composite fields of UV under s-confinement. Moreover, the SM gauge group $G_{\text{SM}} \equiv \text{SU}(3)_C \times \text{SU}(2)_L \times \text{U}(1)_Y$ (including the chiral $\text{SU}(2)_L \times \text{U}(1)_Y$) is preserved *not* spontaneously broken by the s-confinement dynamics.

Recently, the s-confinement is also applied to another problem: the symmetric mass generation (see [6] for an overview) of the SM in four dimensions [7, 8]. It has been previously stressed that there is no obstruction to give masses and energy gaps to all of the SM fermions without breaking the G_{SM} or Grand Unified Theory's internal symmetry as long as there are no anomalies among these internal symmetries [9] (see the systematic checks on the local and global anomaly cancellations for the SM in [10, 11, 12] via cobordism). Ref. [7, 8] provides an explicit model realizing this idea, in the context of the supersymmetric or non-supersymmetric SM. The key idea in [7, 8] is that the *dangerously irrelevant* interaction term in the UV becomes the G_{SM} -preserving *relevant* mass term to achieve the symmetric mass generation in the IR.

Although both Razamat-Tong [7] and our models use the s-confinement dynamics at an intermediate energy scale, the two models (including UV Lagrangian, the deformations, and the IR dynamics) are rather different. In comparison, Ref. [7] considered enlarging from the SM's $15N_f$ or $16N_f$ Weyl fermions to the $27N_f$ Weyl fermions that can be symmetrically gapped out by preserving G_{SM} via a symmetric mass generation deformation, with the family number N_f . Instead, we consider a different UV model with 63 Weyl fermions in total (see Table 1, including the $15N_f$ Weyl fermions in $N_f = 3$ families) with a different deformation. In our scenario, the standard Yukawa coupling at IR corresponds to the higher-scaling-dimensional operator at UV. The G_{SM} -preserving *dangerously irrelevant* higher-scaling-dimensional operator at UV becomes the *marginal* Yukawa coupling at IR. Only when the Higgs field condenses to get a vev at low energy, then the IR dynamics further spontaneously breaks G_{SM} down to the electromagnetic $\text{U}(1)_{\text{EM}}$. This naturally explains the smallness of the first and second family Yukawa couplings, where the smallness is a consequence by the ratio between the s-confinement and cutoff scales (see Fig. 1 (a)). On the other hand, the third family fields are treated as elementary, which is consistent with $\mathcal{O}(1)$ top Yukawa coupling. We present an explicit model to demonstrate the idea. We show that the flavor hierarchy gets milder in our UV model, the coupling of the first and second family (i.e., superpotential coefficients), and the third family Yukawa coupling become closer to $\mathcal{O}(1)$ at high energy. Namely, our UV Lagrangian only contains the natural parameters close to the order one. The

Field	$SU(3)_C$	$SU(2)_L$	$U(1)_Y$	$SU(2)'_1$	$SU(2)'_2$	$U(1)_{B-L}$	$\mathbb{Z}_{4,B-L}$
$L'_{I=1}$	1	2	1/2	2	1	-3	1
$L'_{I=2}$	1	2	1/2	1	2	-3	1
$L_{I=1,2,3}$	1	2	-1/2	1	1	6	2
$D'_{I=1}$	3	1	-1/3	2	1	1	1
$D'_{I=2}$	3	1	-1/3	1	2	1	1
$D_{I=1,2,3}$	$\bar{\mathbf{3}}$	1	1/3	1	1	2	2
$S'_{I=1}$	1	1	0	2	1	3	3
$S'_{I=2}$	1	1	0	1	2	3	3
E_3	1	1	1	1	1	-6	2
U_3	$\bar{\mathbf{3}}$	1	-2/3	1	1	2	2
Q_3	3	2	1/6	1	1	-2	2
H_u	1	2	1/2	1	1	0	0
H_d	1	2	-1/2	1	1	0	0
$\tilde{D}_{I=1,2}$	$\bar{\mathbf{3}}$	1	1/3	1	1	-4	0
$\tilde{L}_{I=1,2}$	1	2	-1/2	1	1	0	0

Table 1: The UV matter contents of superfields of our $\mathcal{N} = 1$ minimal supersymmetric model in the left-handed basis. $U(1)_{B-L}$ is the anomaly free global symmetry, and the last column is $\mathbb{Z}_{4,B-L}$ subgroup of $U(1)_{B-L}$ symmetry. There are 22 Weyl fermions from the chiral multiplets for each of the first and second family ($I = 1, 2$). There are 15 Weyl fermions from the chiral multiplets for the third family ($I = 3$). Each of the two Higgs multiplets introduces 2 Weyl fermions. So the model contains 63 Weyl fermions in total. If we include additional 3 families of right-handed neutrinos neutral to G_{SM} , there will be 66 Weyl fermions in total.

physics at different energy scales from UV to intermediate to IR are shown in Fig. 1 (b).

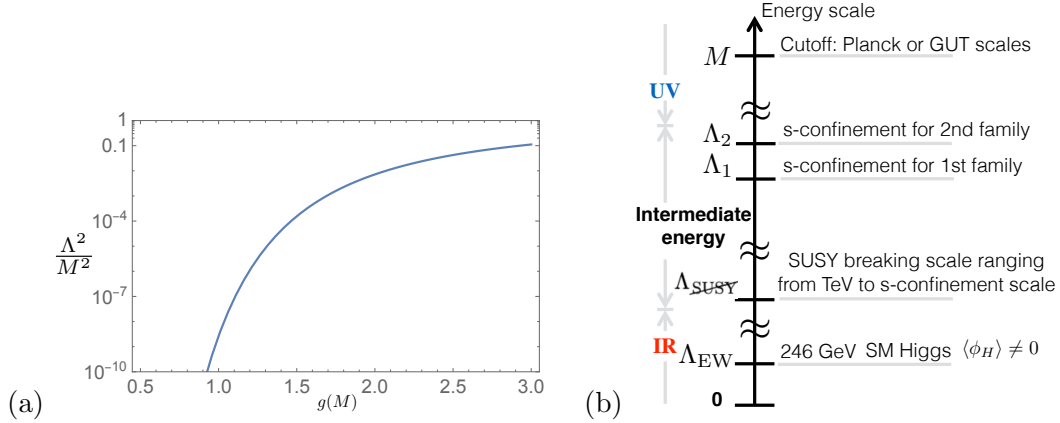


Figure 1: (a) Ratio between the confinement and cutoff scales as a function of the gauge coupling $g(M)$ at the cutoff scale M . This figure reveals that the tiny change of $g(M)$ coupling can correspond to a huge exponential hierarchy between the confinement and the cutoff scales $\frac{\Lambda}{M}$. (b) Physics at different energy scales: The UV Lagrangian is valid somewhere below the cutoff M . The s-confinement happens at intermediate energy Λ_1, Λ_2 while the G_{SM} is still preserved, e.g., $\frac{\Lambda_1}{M}, \frac{\Lambda_2}{M}$ ranges from 10^{-3} to 10^{-1} for phenomenological fitting. Below the supersymmetry breaking scale Λ_{SUSY} , the SM Higgs ϕ_H (given by a linear combination of H_u and H_d) condenses breaking G_{SM} to $U(1)_{EM}$ below Λ_{EW} .

Let us also compare Froggatt-Nielsen model [3] with our model. Froggatt-Nielsen introduced the

flavon field, which suffers from the hierarchy problem associated with the quadratic divergence to the mass squared. Moreover, it is not clear why the vacuum expectation value of the flavon is smaller than the cutoff scale. One of the advantages of our model is that the new hierarchy problem does not occur, since we use s-confinement rather than the Higgs mechanism. The confinement scale appears as the result of the dimensional transmutation, and is naturally smaller than the cutoff scale.

The idea of applying the composite fermions [13] and smooth confinement [4, 5] to fermion mass hierarchy dates back to Strassler [14], Nelson and others [15]. There were also other earlier supersymmetric composite models based on technicolor [16] with similar goals. However, there are significant differences between our model and other previous models: 1. We only require the $SU(3) \times SU(2) \times U(1)$ SM instead of the Grand Unified Theory (GUT) group. 2. We choose the third family fermions elementary, while previous works pursue different routes: such as top-Yukawa-Higgs coupling is dynamically generated, top quark and bottom quark are composite [15]. 3. We choose the large smooth confinement $\Lambda \simeq 10^{-3}M$ to $10^{-1}M$ close to the cutoff scale M , while others choose the much smaller TeV confinement scale [15]. 4. The smooth confinement scale is also the symmetric mass generation scale in our theory, which naturally demands that the coupling strengths of the original SM Lagrangian g_{SM} and the deformation interaction terms g_{int} have an order 1 ratio at our UV theory. This $g_{\text{int}}/g_{\text{SM}} \sim \mathcal{O}(1)$ (or more precisely the energy ratio of the action $E_{\text{int}}/E_{\text{SM}} \sim \mathcal{O}(1)$) is due to the fact that the symmetric energy gap is generated nonperturbatively, so we should *not* rely on a perturbative renormalization group analysis around fixed points at either limit $g_{\text{int}}/g_{\text{SM}} \ll 1$ or $g_{\text{int}}/g_{\text{SM}} \gg 1$.

This article is organized as follows. The UV model is provided in Sec. 2. The model exhibits the s-confinement at the intermediate energy scale, and the minimal supersymmetric SM is realized in the IR, as we show in Sec. 3. We show that the flavor hierarchy is solved by comparing with the experimental data in Sec. 4. The summary and discussions are in Sec. 5.

2 Model in the UV

Inspired by the symmetric mass generation in four dimensions [7], we propose a new model which reduces to the supersymmetric version of the SM in the IR.

The UV matter contents of our model is listed in Table 1. Regarding the first and second families, we introduce the superfields (L'_I, D'_I, S'_I) charged under $SU(2)'_1 \times SU(2)'_2$ ($I = 1, 2$ is the index for the family). There are also superfields $(D_I, \tilde{D}_I, L_I, \tilde{L}_I)$, which are neutral under $SU(2)'_1 \times SU(2)'_2$. As for the third family, the matter contents are the same as those of the $\mathcal{N} = 1$ Minimal Supersymmetric SM, $(Q_3, U_3, D_3, L_3, E_3)$. On top of that, we introduce the Higgs superfields (H_u, H_d) . These are necessary to cancel the dynamical gauge anomaly of $G_{\text{SM}} \equiv SU(3)_C \times SU(2)_L \times U(1)_Y$. In total, there are 63 Weyl fermions in Table 1.

The superpotential of the model is¹

$$\begin{aligned}
W_{\text{UV}} = & y_{IJ}^u \frac{(L'_I D'_I)(D'_J D'_J) H_u}{M^2} + y_{IJ}^d \frac{(L'_I D'_I) D_J H_d}{M} + y_{IJ}^l \frac{L_I (L'_J L'_J) H_d}{M} \\
& + y_{3I}^u \frac{Q_3 (D'_I D'_I) H_u}{M} + y_{I3}^u \frac{(L'_I D'_I) U_3 H_u}{M} + y_{3I}^d Q_3 D_I H_d + y_{I3}^d \frac{(L'_I D'_I) D_3 H_d}{M} \\
& + y_{3I}^l \frac{L_3 (L'_I L'_I) H_d}{M} + y_{I3}^l L_I E_3 H_d + y_{33}^u Q_3 U_3 H_u + y_{33}^d Q_3 D_3 H_d \\
& + y_{33}^l L_3 E_3 H_d + \lambda_I^D \tilde{D}_I (D'_I S'_I) + \mu H_u H_d + \lambda_{IJ}^L \tilde{L}_I (L'_J S'_J)
\end{aligned} \tag{1}$$

where M is the cutoff scale of the model. This could be the GUT or Planck scale. This is the most general superpotential (up to four-fermion interaction terms) which possess $U(1)_{B-L}$ (or its subgroup $\mathbb{Z}_{4,B-L}$) defined in Table 1. As we will see, the $\mathbb{Z}_{4,B-L}$ subgroup of $U(1)_{B-L}$ is identified as matter parity in the Minimal Supersymmetric SM. If we do not impose $U(1)_{B-L}$ or $\mathbb{Z}_{4,B-L}$, the following superpotential is allowed:

$$\begin{aligned}
W_{\Delta L=1,\text{UV}} = & \lambda^{IJK} \frac{L_I L_J (L'_K L'_K)}{M} + \lambda'^{IJK} \frac{L_I (L'_J D'_J) D_K}{M} + \mu'^I L_I H_u + \mu''^{IJ} L_I (L'_J S'_J), \\
W_{\Delta B=1,\text{UV}} = & \lambda''^{IJK} \frac{(D'_I D'_I) D_J D_K}{M}.
\end{aligned} \tag{2}$$

These terms must be small in order to avoid the fast proton decay.

3 Effective theory in the IR

The beta function of $SU(2)'_1 \times SU(2)'_2$ gauge coupling is negative, and therefore the system is strongly coupled at IR, and asymptotic free at UV. The one-loop beta functions of the model is

$$\mu \frac{dg_I}{d\mu} = - \left(\frac{11}{3} C_2(G) - \frac{1}{3} n_s T(R_s) - \frac{2}{3} 2n_f T(R_f) \right) \frac{g_I^3}{16\pi^2} = - \frac{13g_I^3}{48\pi^2}, \quad I = 1, 2. \tag{3}$$

where g_I is the gauge coupling of $SU(2)'_I$ at the energy scale μ , the quadratic Casimir is $C_2(G) = 2$ of $G = SU(2)'_I$. The number of complex scalars $n_s = 6$ and the number of Weyl fermions $2n_f = 6$ that couple to G are all from the 6 chiral multiplets. $T(R_s) = T(R_f) = \frac{1}{2}$ for the fundamental representation. The strongly coupled s-confinement scale Λ_I is

$$\Lambda_I^2 = M^2 \exp \left(- \frac{48\pi^2}{13g_I^2(M)} \right), \tag{4}$$

where $g_I(M)$ is the coupling at the cutoff scale $\mu = M$.

In the IR, the system exhibits the s-confinement [4, 5], which magic requires $n_c + 1 = n_f$ where $n_c = 2$ is from $SU(2)'_I$ and $n_f = 3$ implies the 6 Weyl fermions that couple to the $SU(2)'_I$. The IR fields are the composites of UV fields:

$$E_I \equiv \frac{\epsilon_{ab} L_I^a L_I^b}{\Lambda_I}, \quad U_{kI} \equiv \frac{\epsilon_{ijk} D_I^i D_I^j}{\Lambda_I}, \quad Q_{bI}^i \equiv \frac{\epsilon_{ab} L_I^a D_I^i}{\Lambda_I}, \quad \tilde{D}_I^i \equiv \frac{D_I^i S'_I}{\Lambda_I}, \quad \tilde{L}'_I \equiv \frac{L'_I S'_I}{\Lambda_I}, \tag{5}$$

¹To be precise, more terms are allowed since H_d and \tilde{L}_I have the same quantum number. Similarly, H_u and $L'_I S'_I$ has the same quantum number. In generic situation, the last two terms in Eq. (1) will be 3 by 3 mass matrix in the IR. We assume that one of the linear combination is relatively light, which we call H_u and H_d . The electroweak Higgs is obtained from a linear-combination of H_u and H_d .

where $a, b = 1, 2$ is $SU(2)_L$ index, $i, j, k = 1, 2, 3$ is $SU(3)_C$ index, and Λ_I is the confinement scale of $SU(2)'_I$. The IR matter contents are summarized in Table 2.

At IR low energy below the s-confinement scale, the superpotential (1) becomes

$$\begin{aligned}
W_{\text{IR}} &= y_{IJ}^u \frac{\Lambda_I \Lambda_J}{M^2} Q_I U_J H_u + y_{IJ}^d \frac{\Lambda_I}{M} Q_I D_J H_d + y_{IJ}^l \frac{\Lambda_J}{M} L_I E_J H_d \\
&+ y_{3I}^u \frac{\Lambda_I}{M} Q_3 U_I H_u + y_{I3}^u \frac{\Lambda_I}{M} Q_I U_3 H_u + y_{3I}^d Q_3 D_I H_d + y_{I3}^d \frac{\Lambda_I}{M} Q_I D_3 H_d \\
&+ y_{3I}^l \frac{\Lambda_I}{M} L_3 E_I H_d + y_{I3}^l L_I E_3 H_d + y_{33}^u Q_3 U_3 H_u + y_{33}^d Q_3 D_3 H_d \\
&+ y_{33}^l L_3 E_3 H_d + \mu H_u H_d + \lambda_I^D \Lambda_I \tilde{D}_I \tilde{D}'_I + \lambda_I^L \Lambda_I \tilde{L}_I \tilde{L}'_I \\
&\equiv \tilde{y}_{\alpha\beta}^u Q_\alpha U_\beta H_u + \tilde{y}_{\alpha\beta}^d Q_\alpha D_\beta H_d + \tilde{y}_{\alpha\beta}^l L_\alpha E_\beta H_d + \tilde{\mu} H_u H_d + \tilde{M}_I^D \tilde{D}_I \tilde{D}'_I + \tilde{M}_I^L \tilde{L}_I \tilde{L}'_I,
\end{aligned} \tag{6}$$

where $\alpha, \beta = 1, 2, 3$, while \tilde{y}^u, \tilde{y}^d and \tilde{y}^l are the low-energy Yukawa couplings.

In the IR, Eq. (2) becomes

$$\begin{aligned}
W_{\Delta L=1, \text{IR}} &= \lambda^{IJK} L_I L_J E_K + \lambda'^{IJK} L_I Q_J D_K + \mu^I L_I H_u + \mu'^{IJ} L_I \tilde{L}'_J, \\
W_{\Delta B=1, \text{IR}} &= \lambda''^{IJK} U_I D_J D_K.
\end{aligned} \tag{7}$$

Again, this breaks $U(1)_{B-L}$ and its $\mathbb{Z}_{4, B-L}$ subgroup.

4 Comparison with experimental data

From [17], the experimental data of the Yukawa coupling is²

$$\begin{aligned}
\tilde{y}_{11}^u \sin \beta &\sim 6 \times 10^{-6}, & \tilde{y}_{22}^u \sin \beta &\sim 3 \times 10^{-3}, & \tilde{y}_{33}^u \sin \beta &\sim 0.8, \\
\tilde{y}_{11}^d \cos \beta &\sim 1 \times 10^{-5}, & \tilde{y}_{22}^d \cos \beta &\sim 3 \times 10^{-4}, & \tilde{y}_{33}^d \cos \beta &\sim 1 \times 10^{-2}, \\
\tilde{y}_{11}^l \cos \beta &\sim 3 \times 10^{-6}, & \tilde{y}_{22}^l \cos \beta &\sim 6 \times 10^{-4}, & \tilde{y}_{33}^l \cos \beta &\sim 1 \times 10^{-2}.
\end{aligned} \tag{8}$$

The singular value decompositions of Yukawa coupling \tilde{y}^u and \tilde{y}^d are

$$\tilde{y}^u = U^u \text{diag}(Y_u, Y_c, Y_t) V^u, \quad \tilde{y}^d = U^d \text{diag}(Y_d, Y_s, Y_b) V^d, \tag{9}$$

where $U^{u,d}$ and $V^{u,d}$ are unitary matrices. The CKM matrix is defined as

$$V_{\text{CKM}} = (U^u)^\dagger U^d. \tag{10}$$

The Wolfenstein parametrization of the CKM matrix is

$$V_{\text{CKM}} = \begin{pmatrix} 1 - \frac{1}{2}\lambda^2 & \lambda & A\lambda^3(\rho - i\eta) \\ -\lambda & 1 - \frac{1}{2}\lambda^2 & A\lambda^2 \\ A\lambda^3(1 - \rho - i\eta) & -A\lambda^2 & 1 \end{pmatrix} + \mathcal{O}(\lambda^4), \tag{11}$$

²Here $\tan \beta$ is defined as the ratio of the VEV of two Higgs at the electroweak symmetry breaking vacuum, $\tan \beta \equiv \langle H_u \rangle / \langle H_d \rangle$.

Field	$SU(3)_C$	$SU(2)_L$	$U(1)_Y$	$U(1)_{B-L}$	$\mathbb{Z}_{4,B-L}$	$\mathbb{Z}_{2,\mathbf{R}}$
$E_{I=1,2,3}$	1	1	1	-6	2	1
$U_{I=1,2,3}$	$\bar{\mathbf{3}}$	1	-2/3	2	2	1
$Q_{I=1,2,3}$	3	2	1/6	-2	2	1
$L_{I=1,2,3}$	1	2	-1/2	6	2	1
$D_{I=1,2,3}$	$\bar{\mathbf{3}}$	1	1/3	2	2	1
$\tilde{D}_{I=1,2}$	$\bar{\mathbf{3}}$	1	1/3	-4	0	0
$\tilde{D}'_{I=1,2}$	3	1	-1/3	4	0	0
H_u	1	2	1/2	0	0	0
H_d	1	2	-1/2	0	0	0
\tilde{L}_I	1	2	-1/2	0	0	0
\tilde{L}'_I	1	2	1/2	0	0	0

Table 2: The IR matter contents in the left-handed basis. The IR composite fields are given in Eq. (5). All fields are singlet under $SU(2)'_1 \times SU(2)'_2$. The original $\mathbb{Z}_{4,B-L}$ symmetry is identified as matter-parity $\mathbb{Z}_{2,\mathbf{R}}$ of the minimal supersymmetric standard model (MSSM) [18] in the IR. We can understand that the MSSM's chiral multiplets are composed of two fermions with $\mathbb{Z}_{4,B-L}$ charge 1 from Table 1, which become the IR field with $\mathbb{Z}_{4,B-L}$ charge 2, thus with $\mathbb{Z}_{2,\mathbf{R}}$ charge 1, under the s confinement (via $SU(2)'_1$ and $SU(2)'_2$ dynamical gauge field confinement). Here we have a normal subgroup embedding $\mathbb{Z}_{2,\mathbf{R}} \subset \mathbb{Z}_{4,B-L} \subset U(1)_{B-L}$.

where $\lambda \simeq 0.23$, $A \simeq 0.8$, $\rho \simeq 0.14$ and $\eta \simeq 0.35$. This means that the observed value of CKM matrix is

$$V_{\text{CKM}}^{\text{obs}} \sim \begin{pmatrix} 1 & 0.2 & 0.001 - 0.003i \\ 0.2 & 1 & 0.04 \\ 0.01 - 0.003i & 0.04 & 1 \end{pmatrix}. \quad (12)$$

Similarly, from [17], the experimental value of $Y^{u,c,t}$ and $Y^{d,s,b}$ is

$$\begin{aligned} Y_u^{\text{obs}} &\sim \frac{6 \times 10^{-6}}{\sin \beta}, & Y_c^{\text{obs}} &\sim \frac{3 \times 10^{-3}}{\sin \beta}, & Y_t^{\text{obs}} &\sim \frac{0.8}{\sin \beta}, \\ Y_d^{\text{obs}} &\sim \frac{1 \times 10^{-5}}{\cos \beta}, & Y_s^{\text{obs}} &\sim \frac{3 \times 10^{-4}}{\cos \beta}, & Y_b^{\text{obs}} &\sim \frac{1 \times 10^{-2}}{\cos \beta}, \\ Y_e^{\text{obs}} &\sim \frac{3 \times 10^{-6}}{\cos \beta}, & Y_\mu^{\text{obs}} &\sim \frac{6 \times 10^{-4}}{\cos \beta}, & Y_\tau^{\text{obs}} &\sim \frac{6 \times 10^{-2}}{\cos \beta}. \end{aligned} \quad (13)$$

Let us estimate the Yukawa couplings in our model. From (6), the order of the up and down quark Yukawa couplings are

$$\tilde{y}^u \sim \begin{pmatrix} \frac{\Lambda_1^2}{M^2} & \frac{\Lambda_1 \Lambda_2}{M^2} & \frac{\Lambda_1}{M} \\ \frac{\Lambda_1 \Lambda_2}{M^2} & \frac{\Lambda_2^2}{M^2} & \frac{\Lambda_2}{M} \\ \frac{\Lambda_1}{M} & \frac{\Lambda_2}{M} & 1 \end{pmatrix}, \quad \tilde{y}^d \sim \begin{pmatrix} \frac{\Lambda_1}{M} & \frac{\Lambda_1}{M} & \frac{\Lambda_1}{M} \\ \frac{\Lambda_2}{M} & \frac{\Lambda_2}{M} & \frac{\Lambda_2}{M} \\ 1 & 1 & 1 \end{pmatrix}, \quad (14)$$

while the charged lepton Yukawa coupling is

$$\tilde{y}^l \sim \begin{pmatrix} \frac{\Lambda_1}{M} & \frac{\Lambda_2}{M} & 1 \\ \frac{\Lambda_1}{M} & \frac{\Lambda_2}{M} & 1 \\ \frac{\Lambda_1}{M} & \frac{\Lambda_2}{M} & 1 \end{pmatrix}. \quad (15)$$

By performing the singular value decomposition, we obtain

$$\begin{aligned} Y_u &\sim \frac{\Lambda_1^2}{M^2}, & Y_c &\sim \frac{\Lambda_2^2}{M^2}, & Y_t &\sim 1, \\ Y_d &\sim \frac{\Lambda_1}{M^2}, & Y_s &\sim \frac{\Lambda_2}{M}, & Y_b &\sim 1, \\ Y_e &\sim \frac{\Lambda_1}{M}, & Y_\mu &\sim \frac{\Lambda_2}{M}, & Y_\tau &\sim 1, \end{aligned} \quad (16)$$

and

$$U^u \sim \begin{pmatrix} 1 & \frac{\Lambda_1}{M} & \frac{\Lambda_1}{M} \\ \frac{\Lambda_1}{M} & 1 & \frac{\Lambda_2}{M} \\ \frac{\Lambda_1}{M} & \frac{\Lambda_2}{M} & 1 \end{pmatrix}, \quad U^d \sim \begin{pmatrix} 1 & \frac{\Lambda_1}{\Lambda_2} & \frac{\Lambda_1}{M} \\ \frac{\Lambda_1}{\Lambda_2} & 1 & \frac{\Lambda_2}{M} \\ \frac{\Lambda_1}{M} & \frac{\Lambda_2}{M} & 1 \end{pmatrix}. \quad (17)$$

Then, the CKM matrix is (here $\mathcal{O}(N_1, N_2)$ chooses the maximal among the N_1 and N_2):

$$V_{\text{CKM}} = (U^u)^\dagger U^d \sim \begin{pmatrix} 1 & \mathcal{O}\left(\frac{\Lambda_1}{M}, \frac{\Lambda_1}{\Lambda_2}\right) & \frac{\Lambda_1}{M} \\ \mathcal{O}\left(\frac{\Lambda_1}{M}, \frac{\Lambda_1}{\Lambda_2}\right) & 1 & \frac{\Lambda_2}{M} \\ \frac{\Lambda_1}{M} & \mathcal{O}\left(\frac{\Lambda_2}{M}, \frac{\Lambda_1^2}{M\Lambda_2}\right) & 1 \end{pmatrix}.$$

If we choose

$$\frac{\Lambda_1}{M} \sim 3 \times 10^{-3}, \quad \frac{\Lambda_2}{M} \sim 3 \times 10^{-2}, \quad (18)$$

then, the singular values are

$$\begin{aligned} Y_u &\sim 9 \times 10^{-6}, & Y_c &\sim 9 \times 10^{-4}, & Y_t &\sim 1, \\ Y_d &\sim 3 \times 10^{-3}, & Y_s &\sim 0.03, & Y_b &\sim 1, \\ Y_e &\sim 3 \times 10^{-3}, & Y_\mu &\sim 0.03, & Y_\tau &\sim 1. \end{aligned} \quad (19)$$

and the CKM matrix is

$$V_{\text{CKM}} \sim \begin{pmatrix} 1 & 0.1 & 3 \times 10^{-3} \\ 0.1 & 1 & 0.03 \\ 3 \times 10^{-3} & 0.03 & 1 \end{pmatrix}. \quad (20)$$

By comparing (13) and (19), we observe

$$\begin{aligned}
\frac{Y_u}{Y_u^{\text{obs}}} &\sim 1.5 \sin \beta, & \frac{Y_c}{Y_c^{\text{obs}}} &\sim 0.5 \sin \beta, & \frac{Y_t}{Y_t^{\text{obs}}} &\sim 1 \sin \beta, \\
\frac{Y_d}{Y_d^{\text{obs}}} &\sim 300 \cos \beta, & \frac{Y_s}{Y_s^{\text{obs}}} &\sim 100 \cos \beta, & \frac{Y_b}{Y_b^{\text{obs}}} &\sim 100 \cos \beta, \\
\frac{Y_e}{Y_e^{\text{obs}}} &\sim 10^3 \cos \beta, & \frac{Y_\mu}{Y_\mu^{\text{obs}}} &\sim 50 \cos \beta, & \frac{Y_\tau}{Y_\tau^{\text{obs}}} &\sim 20 \cos \beta.
\end{aligned} \tag{21}$$

Similarly, from (12) and (20), we get the $\mathcal{O}(1)$ ratio between our theoretical fit and the experimental data:

$$\frac{|V_{\text{CKM},IJ}|}{|V_{\text{CKM},IJ}^{\text{obs}}|} \sim \begin{pmatrix} 1 & 2 & 1 \\ 2 & 1 & 1 \\ 3 & 1 & 1 \end{pmatrix}. \tag{22}$$

We observe that the CKM matrix is nicely fitted.

As for the fermion masses, at least the hierarchy is milder than the original SM. If we choose smaller $\cos \beta$, the hierarchy is getting milder. For example, $\cos \beta \sim 0.1$ (so $\tan \beta = 10$) corresponds to $Y_e/Y_e^{\text{obs}} \sim 10^2$, and $\cos \beta \sim 0.02$ (so $\tan \beta = 40$) corresponds to $Y_e/Y_e^{\text{obs}} \sim 20$.³

The neutrino sector is the same as the SM. By adding the right-handed neutrino superfield which is singlet under G_{SM} , we can write down the neutrino Yukawa coupling and Majorana mass:

$$W_N = y_{IJ}^N L_I N_J H_u + M_{IJ} N_I N_J. \tag{23}$$

These terms break continuous $U(1)_{B-L}$ symmetry, but preserves $\mathbb{Z}_{4,B-L}$ symmetry by assigning charge 2 to N_I . Adding 3 right-handed neutrinos would change the model from 63 to 66 Weyl fermions.

After the electroweak symmetry breaking, the neutrino gets the Dirac mass $(M_D)_{IJ} = y_{IJ}^N \langle H_u \rangle$. By integrating out right handed neutrino, the light neutrino mass matrix is

$$(m^\nu)_{IJ} = (m_D)_{IK} (M^{-1})_{KL} (m_D)_{LJ}. \tag{24}$$

This is diagonalized as

$$(m^\nu)_{IJ} = U^\nu \text{diag}(m^{\nu 1}, m^{\nu 2}, m^{\nu 3}) (U^\nu)^T. \tag{25}$$

$$\tilde{y}^e = U^l \text{diag}(Y_e, Y_\mu, Y_\tau) V^l, \tag{26}$$

Then, the PMNS matrix is defined as

$$U_{\text{PMNS}} = U^\nu U^{l\dagger} = \begin{pmatrix} c_{12}c_{13} & s_{12}c_{13} & s_{13}e^{-i\delta_{CP}} \\ -s_{12}c_{23} - c_{12}s_{23}s_{13}e^{i\delta_{CP}} & c_{12}c_{23} - s_{12}s_{23}s_{13}e^{i\delta_{CP}} & s_{23}c_{13} \\ s_{12}s_{23} - c_{12}c_{23}s_{13}e^{i\delta_{CP}} & -c_{12}s_{23} - s_{12}c_{23}s_{13}e^{i\delta_{CP}} & c_{23}c_{13} \end{pmatrix}, \tag{27}$$

where $s_{IJ} = \sin \theta_{IJ}$, $c_{IJ} = \cos \theta_{IJ}$ are the mixing angles, and δ_{CP} is the CP phase. The matrix V^ℓ is constrained by the charge assignment in our model, whereas the matrix U^ℓ is arbitrary. Therefore, the experimental data is fitted by choosing U^ν appropriately. Beware that our model has not yet explained the smallness of the mixing angle θ_{13} , which may require a mechanism other than the one we propose.

³Roughly speaking, the large $\tan \beta$ corresponds to a smaller supersymmetry breaking scale. Given the bound from LHC, the value of $\tan \beta$ cannot be much bigger than 50.

5 Summary

We have proposed a new mechanism involving the s-confinement to explain the flavor hierarchy in the Standard Model. The s-confinement dynamics is used to drive the *dangerously irrelevant* higher-scaling-dimensional operators at UV to the *marginal* Yukawa-Higgs deformation at IR in our model. (In contrast, the s-confinement is used differently in the symmetric mass generation deformation in [7, 8].) The smallness of the Yukawa coupling in the flavor hierarchy problem is explained as the ratio of the s-confinement and the cutoff scales. We propose an explicit supersymmetric model to resolve the flavor hierarchy with the $\mathcal{O}(1)$ coefficients at UV. The UV Lagrangian is more consistent with Dirac or 't Hooft criteria on the naturalness [19]. In fact, when the SMG happens, the relative strengths between the Standard Model action S_{SM} and the SMG interaction action $gS_{\text{SMG,int}}$ together $S_{\text{SM}} + gS_{\text{SMG,int}}$ have the dimensionless coupling ratio $g \simeq \mathcal{O}(1)$ of the naturalness order 1 (Also $|\frac{E_{\text{SMG,int}}}{E_{\text{SM}}}| \sim \mathcal{O}(1)$ for the energy ratios) [20, 21]. So in fact the SMG types of processes demand Naturalness!

Some comments and promising future directions follow.

1. It will be interesting to investigate both the supersymmetric and non-supersymmetric scenarios of the models similar to ours for the flavor hierarchy resolution.

2. One can also consider the symmetric mass generation deformation of our 63 or 66 Weyl fermion model. One can also enlarge our model to include also the $27N_f$ Weyl fermion model of [7], so to introduce both the symmetric mass generation and Yukawa-Higgs deformations under the umbrella of a parent theory. One can study the phase transitions between different phases of the parent theory [22].

3. The symmetric mass generation in [7, 8] still allows a *mean-field* fermion bilinear mass term description at IR, although this mean-field mass does not break G_{SM} because that the G_{SM} is redefined when the matter contents are enlarged by adding more fields from UV. However, a more intrinsic symmetric mass generation requires a *non-mean-field* mass deformation, purely driven by the multi-field interactions or the disorder mass field configurations [6, 23, 24] — this alternative *beyond-mean-field* deformation deserves future study [24].

4. The large $\tan \beta$ mildens the flavor hierarchy, but the $\tan \beta$ cannot be too large otherwise it lowers supersymmetry breaking scale that violates the experimental bound. It will be desirable to sharpen the rough constraint [25] $\tan \beta < 50$ here to find the future phenomenology evidence.

5. The s-confinement scenario has the asymptotic freedom at the deep UV $\gg \Lambda$, while the higher-scaling-dimensional operator and multi-field interaction are nonrenormalizable becoming nonperturbatively strong also at UV approaching to the cutoff scale M . Closer to the cutoff M challenges the validity of the effective field theory, it is worthwhile to find, in addition to the discrete lattice formulation, any alternative continuum UV completion of our model.

6. As a condensed matter application, the (iso)spin and the electrically charged degrees of freedom can be separated by a larger energy gap. It will be interesting to know if the smooth confinement analogy works or not to explain the (iso)spin-charge separation hierarchy.

Acknowledgment

The work of YH was supported by Japan Society for the Promotion of Science (JSPS) Overseas Research Fellowships. At the final stages of the work, YH was supported by MEXT Leading Initiative for Excellent Young Researchers Grant Number JPMXS0320210099. The work of JW is supported by Harvard University CMSA. JW thanks the participants of Generalized Global Symmetries workshop (September 19-23, 2022) at Simons Center for Geometry and Physics for the inspiring program. After the manuscript submission, we are grateful to receive helpful comments from Nathan Seiberg and Matthew Strassler.

References

- [1] Particle Data Group, P. A. Zyla et al., *Review of Particle Physics*, PTEP **2020** (2020), no. 8, 083C01.
- [2] J. de Blas, M. Pierini, L. Reina, and L. Silvestrini, *Impact of the recent measurements of the top-quark and W-boson masses on electroweak precision fits*, (2022), 2204.04204.
- [3] C. D. Froggatt and H. B. Nielsen, *Hierarchy of Quark Masses, Cabibbo Angles and CP Violation*, Nucl. Phys. B **147** (1979), 277–298.
- [4] N. Seiberg, *Exact results on the space of vacua of four-dimensional SUSY gauge theories*, Phys. Rev. D **49** (1994), 6857–6863, hep-th/9402044.
- [5] N. Seiberg, *Electric - magnetic duality in supersymmetric nonAbelian gauge theories*, Nucl. Phys. B **435** (1995), 129–146, hep-th/9411149.
- [6] J. Wang and Y.-Z. You, *Symmetric Mass Generation*, Symmetry **14** (2022), no. 7, 1475, 2204.14271.
- [7] S. S. Razamat and D. Tong, *Gapped Chiral Fermions*, Phys. Rev. X **11** (2021), no. 1, 011063, 2009.05037.
- [8] D. Tong, *Comments on symmetric mass generation in 2d and 4d*, JHEP **07** (2022), 001, 2104.03997.
- [9] J. Wang and X.-G. Wen, *A Non-Perturbative Definition of the Standard Models*, Phys. Rev. Res. **2** (2020), no. 2, 023356, 1809.11171.
- [10] I. Garcia-Etxebarria and M. Montero, *Dai-Freed anomalies in particle physics*, JHEP **08** (2019), 003, 1808.00009.
- [11] J. Davighi, B. Gripaios, and N. Lohitsiri, *Global anomalies in the Standard Model(s) and Beyond*, JHEP **07** (2020), 232, 1910.11277.
- [12] Z. Wan and J. Wang, *Beyond Standard Models and Grand Unifications: Anomalies, Topological Terms, and Dynamical Constraints via Cobordisms*, JHEP **07** (2020), 062, 1910.14668.
- [13] S. Dimopoulos, S. Raby, and L. Susskind, *Light Composite Fermions*, Nucl. Phys. B **173** (1980), 208–228.
- [14] M. J. Strassler, *Generating a fermion mass hierarchy in a composite supersymmetric standard model*, Phys. Lett. B **376** (1996), 119–126, hep-ph/9510342.

- [15] A. E. Nelson and M. J. Strassler, *A Realistic supersymmetric model with composite quarks*, Phys. Rev. D **56** (1997), 4226–4237, hep-ph/9607362.
- [16] E. Farhi and L. Susskind, *Technicolor*, Phys. Rept. **74** (1981), 277.
- [17] S. Antusch and V. Maurer, *Running quark and lepton parameters at various scales*, JHEP **11** (2013), 115, 1306.6879.
- [18] S. P. Martin, *A Supersymmetry primer*, Adv. Ser. Direct. High Energy Phys. **18** (1998), 1–98, hep-ph/9709356.
- [19] G. 't Hooft, *Naturalness, chiral symmetry, and spontaneous chiral symmetry breaking*, NATO Sci. Ser. B **59** (1980), 135–157.
- [20] J. Wang and X.-G. Wen, *Nonperturbative regularization of (1+1)-dimensional anomaly-free chiral fermions and bosons: On the equivalence of anomaly matching conditions and boundary gapping rules*, Phys. Rev. B **107** (2023), no. 1, 014311, 1307.7480.
- [21] M. Zeng, Z. Zhu, J. Wang, and Y.-Z. You, *Symmetric Mass Generation in the 1+1 Dimensional Chiral Fermion 3-4-5-0 Model*, Phys. Rev. Lett. **128** (2022), no. 18, 185301, 2202.12355.
- [22] J. Wang, Z. Wan, and Y.-Z. You, *Cobordism and deformation class of the standard model*, Phys. Rev. D **106** (2022), no. 4, L041701, 2112.14765.
- [23] J. Wang, *CT or P problem and symmetric gapped fermion solution*, Phys. Rev. D **106** (2022), no. 12, 125007, 2207.14813.
- [24] J. Wang, *Strong CP Problem and Symmetric Interacting Mass Solution*, (2022), 2212.14036.
- [25] G. Degrandi, S. Di Vita, J. Elias-Miro, J. R. Espinosa, G. F. Giudice, G. Isidori, and A. Strumia, *Higgs mass and vacuum stability in the Standard Model at NNLO*, JHEP **08** (2012), 098, 1205.6497.